Synthesis and biological evaluation of FJ-809, a compound originally described as MIM1 and inhibitor of the anti-apoptotic protein Mcl-1

Frédéric Justaud, Hippolyte Paysant, Louis Bastien Weiswald, Abdelghani Jebahi, Marie Jouanne, Nicolas Elie, Anne Sophie Voisin-Chiret, Thierry Roisnel, Clément Orionne, Nicolas Levoin, et al.

Synthesis and biological evaluation of FJ-809, a compound originally described as MIM1 and inhibitor of the anti-apoptotic protein Mcl-1.

Frédéric Justaud,[1] Hippolyte Paysant,[2,3] Louis Bastien Weiswald,[2,3] Abdelghani Jebahi,[2,3] Marie Jouanne,[4] Nicolas Elie,[5] Anne Sophie Voisin-Chiret,[4] Thierry Roisnel,[1] Clément Orionne,[6] Nicolas Levoin,[7] Laurent Poulain[2,3] and René Grée[1*]

The development of inhibitors of anti-apoptotic proteins, such as Mcl-1, is currently a very active area in the field of cancer research. One of the very first reported inhibitor of Mcl-1 was the molecule **MIM1**, but we have demonstrated recently that the structure of this compound had to be revised from **2** to the derivative **1 (FJ-809)**. In this paper we first develop a strategy to prepare unambiguously molecules such as **1** with a thiazol-3(2H)-yl)imino core, instead of the [2(3*H*)-thiazolylidene]hydrazine previously found in **MIM1** (**2**). Next a series of biological studies have been performed on **1**, using IGROV1-R10 ovarian cancer cells as models, and they have been complemented by Fluorescence Polarisation Assays. These studies demonstrated that the new compound **FJ-809 (1)** was devoid of any significant activity on Mcl-1, contrary to **2**. Then molecular modelling and molecular dynamic studies have been performed in order to elucidate the differences between **FJ-809** and **MIM1** in their interaction with the Mcl-1 protein.

Keywords: cancer; anti-apoptotic proteins; Mcl-1; MIM1; thiazoles; bioassays; molecular modelling.

Introduction

Cancers are responsible for nearly 10 million deaths in 2020,[1] and overcoming resistance of cancer cells to conventional treatment is a major challenge in oncology. As one of the hallmarks of cancer,[2] deregulation of apoptosis is frequent, both in carcinogenesis and chemoresistance, thus the development of innovative pro-apoptotic strategies appears as a key issue in cancer research. Bcl-2 family proteins have critical roles in the control of apoptosis and its anti-apoptotic relatives i.e. Bcl-xl, Mcl-1, Bcl-w and Bfl1/A1, are overexpressed in various hematopoietic and solid tumors.[3] They are known to contribute to cancer development and therapy resistance and development of strategies aiming at inhibiting these anti-apoptotic proteins is therefore an intensive area of research in medicinal chemistry. This led to the design of small molecules able to target these proteins and the development of Venetoclax (ABT-199), the first-in-class targeted medicine designed to selectively inhibit Bcl-2 and approved by the Food and Drug Administration (FDA).[4] Considerable efforts are currently being made to develop inhibitors of Mcl-1 since its overexpression is often detected in many tumor types and is associated with tumorigenesis, poor prognosis and drug resistance,[5a] including resistance to Bcl-2/Bcl-x_L inhibitors. Several compounds [S64315 (Servier), AMG176 (Amgen) and AZD5991 (AstraZeneca)] have entered phase 1 clinical trials involving patients with hematological malignancies.[6] Among Mcl-1 inhibitors already described,[7] **MIM1** (**2**, Figure 1) is a small molecule first identified by virtual screening of a 71296 members chemical library and then by a stapled peptide-based competitive screen. Further, this molecule was proved to selectively bind and inhibit the BH3-binding groove of Mcl-1[8] and it has often been used as a reference in biological studies.

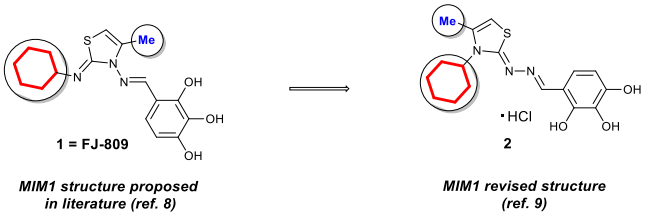

Fig. 1 Structures of **FJ-809** (**1**) and **MIM1** (**2**)

We have demonstrated recently that the structure **1**, initially proposed for **MIM1**, was not exact and we have revised it to compound **2** (Fig. 1). Further, we have designed and synthetized a focused library of analogues of **2**. Then in vitro and in cellulo biological experiments, combined with extensive molecular modelling studies, allowed us to propose preliminary Structure-Activity Relationships for these series of molecules.[9]

To complete previous studies we decided to prepare, by an independent route, the compound with the structure attributed to **1** and study its chemical and biological properties, in comparison with **MIM1** (**2**). Thus, the goal of this paper is to report an unambiguous synthesis of compound **1**, that we will name **FJ-809** to avoid any confusion with corrected **MIM1** (**2**). Besides showing analytical and physical properties clearly different from **2**, this molecule **FJ-809** exhibit also different biological properties as described in the second part of this paper. A rationale for such differences will be proposed based on molecular modelling and molecular dynamic studies.

Results and discussion

- **Chemical Synthesis**

The reaction of thiosemicarbazides with β-halogeno ketones is the classical method employed for the preparation of this type of thiazole-derived heterocycles. As indicated in Scheme 1, it could lead to two types of structures, either a thiazol-3(2H)-yl)imino core **6** if the nitrogen of the hydrazone group is concerned by the cyclization (pathway 1) or a [2(3*H*)-thiazolylidene]hydrazone **7** if the terminal nitrogen is involved (pathway 2). We have shown that, in the case of **MIM1** synthesis where **R²** = aryl groups, the second pathway is involved affording the type-**7** structures. This was the background for the correction of **MIM1** structure.

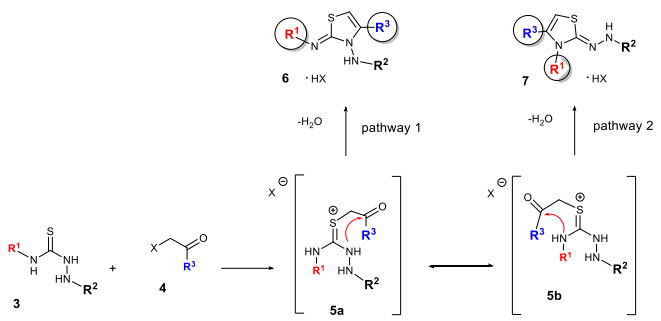

Scheme 1 Synthesis of type-**6** and type-**7** heterocycles

On the other hand, it has been described in the literature that when **R²** is H or an alkyl group the pathway 1 is occurring,[10] and similar result was obtained if **R²** is a COPh.[11] Based on this information, for the synthesis of compound **FJ-809** with the originally assigned structure **1**, we designed a strategy using a Boc group in **R²** position and this was performed according to Scheme 2:

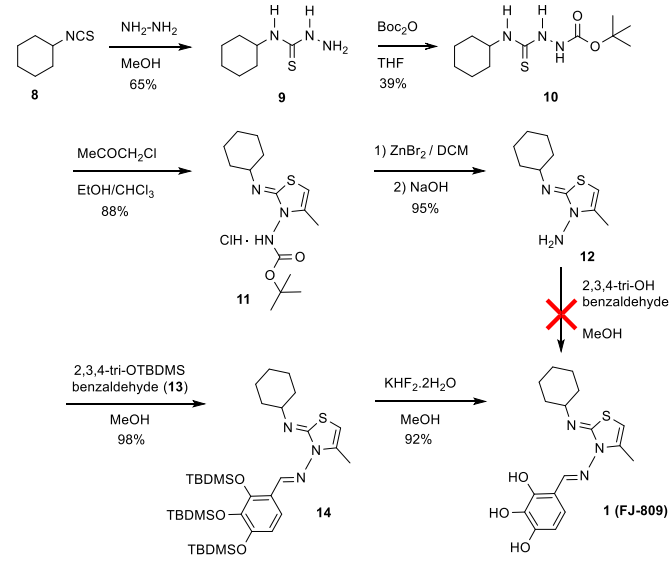

Scheme 2 Synthesis of the target molecule **FJ-809**.

The known thiourea **9,** obtained by condensation of cyclohexyl-isothiocyanate **8** with aqueous hydrazine, was protected as the *N*-Boc derivative **10** in a moderate yield. The heterocyclization was performed by reaction of **10** with chloroacetone in an ethanol-chloroform mixture at 65°C, affording in 88% yield the derivative **11**, as an hydrochloride salt. Deprotection by zinc bromide in dichloromethane at room temperature, followed by an alcaline wash gave the neutral intermediate **12** in 95% yield. Acidic conditions have to be avoided since they led to degradation. The direct condensation of **12** with 2,3,4-trihydroxybenzaldehyde proved to be unsuccessfull and in most cases, no reaction took place. Different Lewis acids, molecular sieves, drying agents and/or different solvents were tried without success and increase of the temperature led to degradation. Therefore, we replaced the triphenol intermediate by the known,[12] trisOTMBS protected derivative **13**. Then the condensation went on smoothly, affording **14** in 98% yield. The final deprotection step was not straightforward but after trying various conditions, it was found that using an excess of $KHF_2.H_2O$ in methanol at room temperature, the target molecule **1** (**FJ-809)** could be isolated in 92% yield. Thus, **FJ-809** was obtained under mild conditions in 6 steps and 19% overall yield from **8**.

All these molecules have spectral and analytical data (see experimental section and ESI) consistent with their structure. Most informative are the comparison of the NMR data of **1** (**FJ-809**) with those (already reported)[9] of the **MIM1** molecule **2**. The ^1H NMR spectrum of a 1:1 mixture of both compounds (Fig. 2) clearly illustrates these differences. In particular, the signals of the protons of the C**H**=N- groups are very different: they appear at 10.2 ppm for **FJ-809** and at 8.2 ppm in the case of **2**. Further, contrary to the results obtained in the case of **2**, no NOESY correlation was observed between the methyl group on the heterocycle and the C**H** and the CH_2 protons of the cyclohexyl substituent of **FJ-809** (see ESI). This was anticipated, taking into account the long distance between these groups in such a thiazol-3(2H)-yl)imino core.

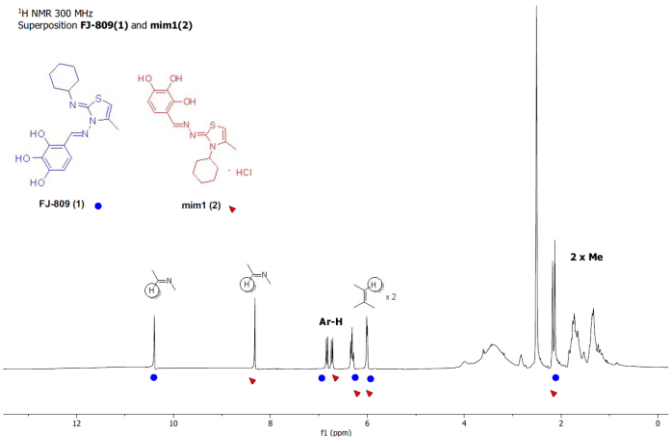

Fig. 2 ^1H NMR spectrum of a 1:1 mixture of **1** (**FJ-809)** and **2** **(MIM1)**.

In spite of many experiments, it was not possible to grew crystals of **FJ-809** suitable for X-Ray analysis. However, starting from the key intermediate **12,** we could prepare two analogues as indicated in Scheme 3.

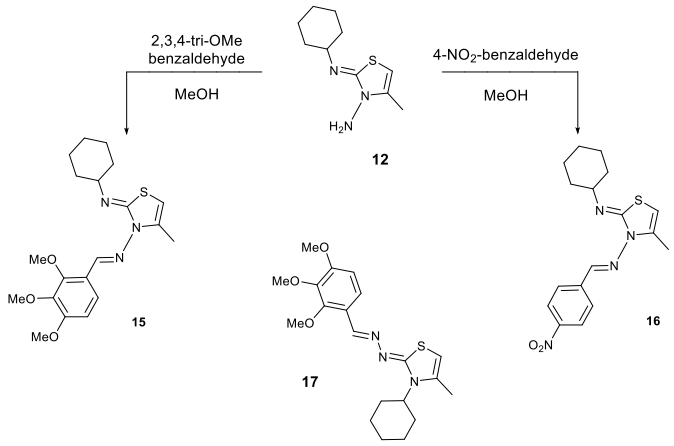

Scheme 3 Synthesis of the analogues **15** and **16**.

The reaction with 2,3,4-trimethoxy-benzaldehyde and with the 4-nitrobenzaldehyde gave the molecules **15** and **16** in 76 and 71% yields, respectively. The physical and analytical data of these derivatives are similar to those of **FJ-809** and consistent with the indicated structures. Further, in the case of **15**, they are clearly different from those of **17** (see for instance the ^{1}H NMR spectrum of the 1:1 mixture of **15** and **17**, Fig. 1 in ESI), the trimethoxy analogue of **2** that we have described recently.[9] Finally, in the case of **16**, the structure was unambiguously

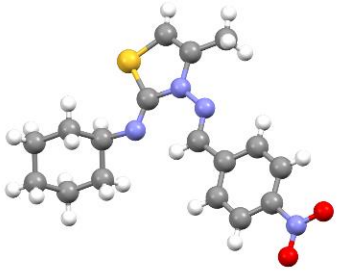

Fig. 3 Structure of compound **16** by X-Ray analysis.

confirmed by X-Ray diffraction analysis as indicated in Figure 3.[13]

Therefore, we have designed a new strategy, based on the use of a *N*-Boc-protected thiourea, which should allow the preparation of many heterocyclic molecules bearing a thiazol-3(2H)-yl)imino core.

- **Biological studies**

We compared the activity of the two molecules **1** and **2** on IGROV1-R10 ovarian cancer cells, whose survival is dependent on both Bcl-x_L and Mcl-1, as described previously.[9] In these cells, the concomitant inhibition of these two anti-apoptotic proteins leads to massive cell apoptotic death. It thus constitutes a pertinent model in the context of Bcl-x_L/Mcl-1 inhibitors screening studies. The cells are exposed simultaneously to the candidate molecules and to a known Bcl-x_L inhibitor (ABT-737). When apoptosis is observed in presence of ABT-737, the molecule is identified as a possible Mcl-1 inhibitor (to be confirmed by other approaches).

Here we showed (Fig. 4) in this model that **MIM1** (**2**) exerts a modest activity on IGROV1-R10 cells at 10µM in combination with ABT-737, as previously described,[9] suggesting its Mcl-1 inhibitor properties, as expected. Cell detachment and nuclear condensations or fragmentations are observed after a 24h exposure to **MIM1** (**2)** (13% at 10µM, Fig. 4, and 18% at 25µM, see Fig. S1 in ESI), as well as a slight caspase 3 cleavage and a strong PARP cleavage in western blot experiments, observed at 10µM.

In contrast, none of these events were observed after exposure to **FJ-809** (**1**) (Fig.4), even at a high concentration (25µM, Fig. S3 in ESI), when combined to ABT-737, suggesting that this molecule is inactive.

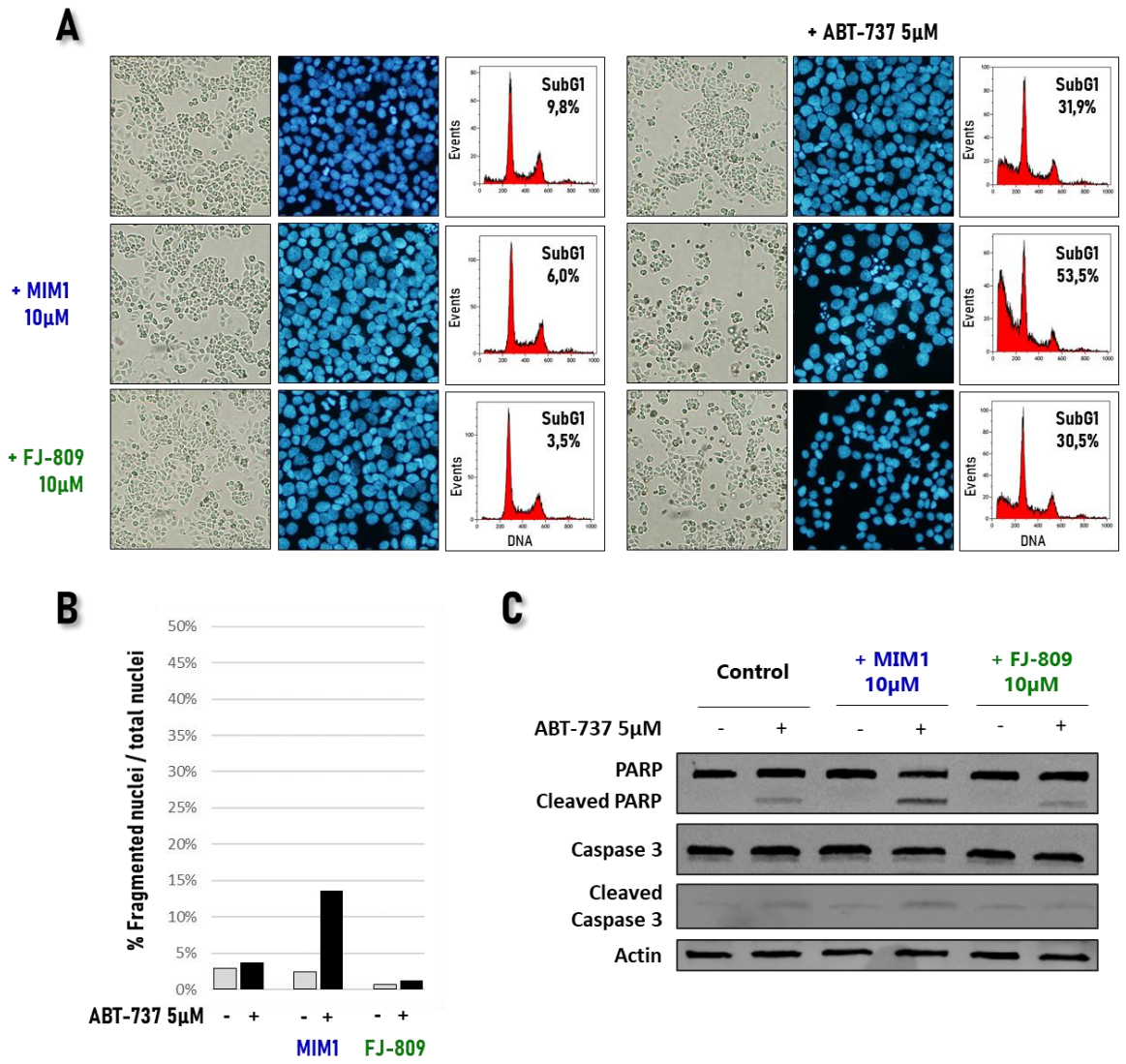

Fig. 4 Evaluation of the biological effect of **MIM1 (2)** and **FJ-809 (1**) on IGROV1-R10 cell line IGROV1-R10 chemoresistant ovarian cancer cell line. This cell line was exposed to either **MIM1** or **FJ-809** (10µM) combined, or not, with ABT-737 (5µM). Effect on cellular and nuclear morphology, as well as cell cycle repartition, is represented (A) and nuclei fragmentation is quantified as described in the experimental section (B). PARP and Caspase 3 cleavage is evaluated by western blot (C).

To complete our result, Fluorescence Polarization Assay (FPA) was performed to elucidate the direct interaction between **MIM1** (**2**) and Mcl-1, or between **FJ-809** (**1**) and Mcl-1. The docking assay shows a Ki=2.6µM for **MIM1** (**2**) towards Mcl-1 (Fig. 5), confirming the results of our previous study. In a similar manner, **FJ-809** (**1**) weakly binds to Mcl-1 (Ki = 13.3µM, Fig. 5), confirming the absence of effect observed on IGROV1-R10 cell line at 10µM (Fig. 4) and 25µM when combined to ABT-737 (5µM) (Fig. S3 in ESI).

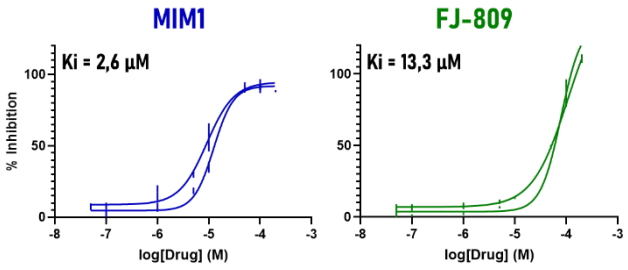

Fig. 5 Binding affinities of **2** (**MIM1)** and **1** (**FJ-809**) on Mcl-1 assessed by Fluorescence Polarization Assay. Ki was extrapolated from both **MIM1** (2.6µM) and **FJ-809** (13.3µM) inhibition percentages values (n=2 for each calculation).

Comparison of FJ-809 and MIM1 by molecular simulations

As we already described,[9] the binding mode of **FJ-809** and **MIM1** are very similar (Fig. 6), with conserved interaction features (van der Waals contacts for the core, hydrogen bonds for the triphenol). Even if the ligand chemical structure was erroneous, the binding mode suggested by Cohen et al,[8a] based on docking and NMR chemical shifts is still valid for both inhibitors. In particular, amino acids located at the C-t end of helix α3 (K234, D236), the N-t part of helix α4 (D241), in the crevice between the two helices (M231, L235, F270), and D256, are either in direct interaction or very close to the ligands. The main difference is that the methyl of **FJ-809** is partially solvent exposed, while the methyl of **MIM1** is more favourably buried in the hydrophobic cavity. In agreement with this observation, interaction energy of the docking pose calculated by a MM-GBSA method showed that **MIM1** has clearly a higher affinity than **FJ-809**: -56.6 vs. -34 kcal/mol.

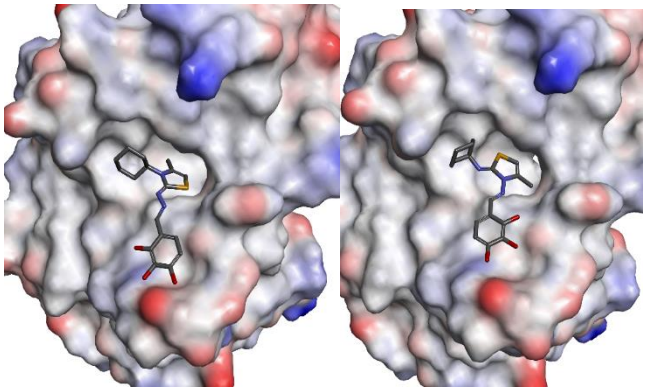

Fig. 6 **MIM1** (**2**, left) and **FJ-809** (**1**, right) bound to Mcl-1, as suggested by molecular docking.

By running molecular dynamics experiments, we noticed that the ligands were movable within the binding pocket, particularly the triphenol group which appeared to be able to form different hydrogen bonds with several amino acids. To reach a more quantitative understanding of the inhibitors interaction with Mcl-1, we performed extensive molecular simulations, by means of five independent µs molecular dynamics of each complex (see SI Fig. S22). Contrary to our intuition, **MIM1** appeared less stationary than **FJ-809**, or rather to fluctuate between a few alternate binding modes (Fig. 7). In Fig. 7A for example, root-mean-square deviation (RMSD) of the ligand showed recurrent fast shifts of the binding mode. During another experiment (Fig. 7B), the initial (t < 100 ns) and late sates (t = 800-900 ns) seemed similar, while the ligand was stable in another binding mode for most the simulation (t = 150-650 ns). On the contrary, **FJ-809** appeared static (Fig. 7C).

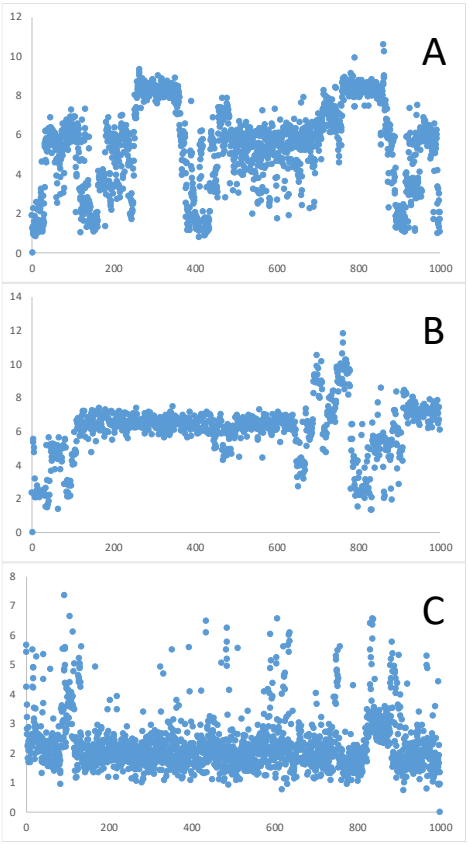

Fig. 7 Fluctuation of **MIM1** and **FJ-809** bound to Mcl-1 (RMSD in Å vs. time in ns). For **MIM1**, the occurrence of different binding mode is highlighted by the RMSD calculated during two independent molecular dynamics experiments (A, B). By contrast, **FJ-809** appears nearly motionless in the binding site (C).

A detailed analysis of the trajectories suggested that this is probably due to the solvent exposure of the **FJ-809** methyl group, which creates an indirect additional attachment point in the pocket. This is the consequence of its first hydration shell which disrupts the hydrogen bond network of water molecules above the binding site and freeze them as a clathrate, as illustrated by the radial distribution function (RDF) between the methyl and water molecules. This behavior is not possible for **MIM1**'s methyl group since it is buried in the binding pocket (Fig. 8).

Hence the flexibility of **MIM1**, for which the entropic cost of binding is reduced, as well as the perturbation of the solvent near **FJ-809** explain the higher affinity of **MIM1**.

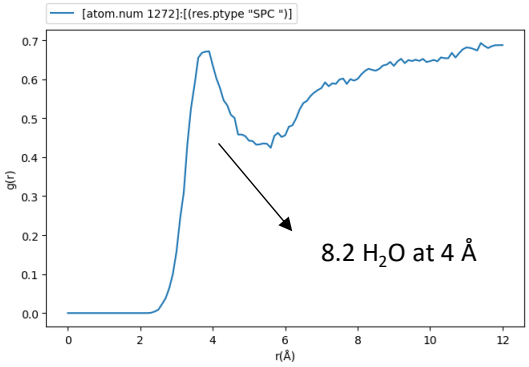

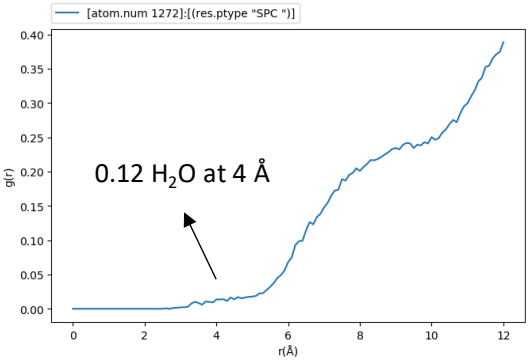

nethyl
lecular
ıe RDF
ere 8.8

Experimental

Chemistry

General informations

NMR spectra were performed on a Bruker AVANCE 300, AVANCE 400 (^{1}H at 300 or 400 MHz; ^{13}C at 75 or 100 MHz). Solvent peaks were used as reference values with $CDCl_3$ at 7.26 ppm for ^{1}H NMR and 77.16 ppm for ^{13}C NMR, with MeOD at 4.78 and 3.31 ppm for ^{1}H NMR and 49.00 ppm for ^{13}C NMR, Chemical shifts δ are given in ppm, and the following abbreviations are used: singlet (s), broad singlet (bs), doublet (d), doublet of doublet (dd), doublet of doublet of doublet (ddd), triplet (t), triplet of doublet (td), quadruplet (q), doublet of quadruplet (dq), and multiplet (m).

IR spectra were recorded on a Perkin Elmer apparatus using a Universal ATR Sampling Accessory and spectra were analysed with spectragryph 1,2,4 version. High resolution mass spectra were recorded in the Centre Régional de Mesures Physiques de l'Ouest, Rennes (CRMPO), on a Maxis 4G. Reaction courses and product mixtures were routinely monitored by TLC on silica gel (precoated F254 Merck plates), and compounds were visualised under a UVP Mineralight UVGL-58 lamp (254 nm) and with *p*-anisaldehyde or $KMnO_4$/Δ. Column chromatography was performed using silica gel 60 (40−63 mm, 230−400 mesh). Solvents were used as received from commercial sources. Reagents were purchased from Sigma-Aldrich, Alfa Aesar and Acros. All corresponding products showed ^{1}H, and ^{13}C NMR spectra in agreement with the assigned structures.

Compound **8** was purchased from Alfa Aesar supplier and used as received.

N-cyclohexylhydrazinecarbothioamide (9)

This compound **9** has been prepared according to reported procedures and its spectral data are in agreement with literature.[14]

tert-butyl 2-(cyclohexylcarbamothioyl)hydrazinecarboxylate (10)

A solution of Boc_2O (358 mg, 1.64 ml, 1.0 equiv.) in THF (8.0 mL) was added to a solution of thiosemicarbazide **9** (346 mg, 1.64 ml, 1.0 equiv.) in THF (8.0 mL) cooled at 0 °C. After complete dissolution within 2 min, the solution was stirred for 12 h. Then, saturated aqueous $NaHCO_3$ solution (15 mL) was added and the mixture extracted with DCM (3 x 50 mL). The combined organic extracts were washed with 0.1 N aqueous HCl (3 x 100 mL), dried over $MgSO_4$ and the volatiles removed by rotary evaporator. The crude mixture was purified by column chromatography using Silica 60-M with DCM/MeOH: 98/2 as eluant to afford 9 (178 mg, 39% yield) of colourless liquescent solid. FTIR (thin film) ν_{max}/cm^{-1} 3333, 3295, 3139, 2926, 2852, 1624, 1522, 1499, 1232, 931. ^{1}H NMR (300 MHz, Chloroform-*d*) δ 7.88 (s, 1H), 6.97 (s, 1H), 6.67 (d, d, *J* = 8.3 Hz, 1H), 4.34 – 4.13 (m, 1H), 2.12 – 1.99 (m, 2H), 1.81 – 1.59 (m, 4H), 1.50 (s, 9H), 1.47 – 1.34 (m, 2H), 1.29 – 1.15 (m, 2H). ^{13}C NMR (75 MHz, $CDCl_3$) δ 181.63, 155.44, 82.74, 53.35, 32.51, 28.11, 25.40, 24.78. HRMS (ESI): calcd for $C_{12}H_{23}N_3O_2SNa$: $[M + Na]^+$: *m/z* 296.14032. Found 296.1402 (0 ppm).

(Z)-tert-butyl (2-(cyclohexylimino)-4-methylthiazol-3(2H)-yl) carbamate hydrochloride (11)

A mixture of the thiosemicarbazide **10** (124 mg, 0.454 mmol, 1.0 equiv.) and chloroacetone (72 µL, 0.910 mmol, 2.0 equiv.) in 7:3 ethanol/chloroform mixture (2.0 ml) was refluxed for 6 h. Then, the mixture was concentrated under vacuum. The foam obtained was dissolved in diethyl ether before evaporation to remove excess of chloroacetone and the process repeated 3 times. The brown foam obtained was used without further purification (140 mg, 88%). FTIR (thin film) ν_{max}/cm^{-1} 3298, 3134, 2928, 2853, 1713, 1532, 1448, 1366, 1220, 1182. ^{1}H NMR (300 MHz, Chloroform-*d*) δ 11.07 (s, 1H), 10.52 (d, *J* = 7.6 Hz, 1H), 6.33 (s, 1H), 3.27 – 3.02 (m, 1H), 2.13 (s, 3H), 2.09 – 2.01 (m, 1H), 1.96 – 1.50 (m, 6H), 1.46 (s, 9H), 1.34 – 1.13 (m, 4H). ^{13}C NMR (75 MHz, $CDCl_3$) δ 167.67, 153.75, 139.96, 97.52, 83.77, 58.84, 31.61, 30.73, 24.67, 24.40, 13.07. HRMS (ESI): calcd for $C_{15}H_{26}N_3O_2S$: $[M + H]^+$: *m/z* 312.17402. Found 312.1740 (0 ppm).

Synthesis of 2-cyclohexylimino-4-methyl-2,3-dihydro-1,3-thiazol-3-amine (12)

To a stirred solution of **11** (765 mg, 2.17 mmol, 1.0 equiv.) in DCM (25 mL) was added by portion zinc bromide (2.44 g, 10.85 mmol, 5.0 equiv.) with rapid solubilisation and decoloration of the solution, further stirred for 3 h at RT. Then, water (20 mL) was added followed by NaOH solution, (2.0 N, 25 mL). The organic layer was collected, dried over $MgSO_4$ and concentrated under vacuo to yield **12** (434 mg, 95% yield) of a pale yellow oil. FTIR (thin film) ν_{max}/cm^{-1} 3244, 3096, 3094, 2922, 2849, 1639, 1610, 1586, 1397, 967. ^{1}H NMR (300 MHz, Chloroform-*d*) δ 6.33 – 5.87 (m, 3H), 3.23 – 3.08 (m, 1H), 2.34 (d, *J* = 1.3 Hz, 3H), 2.09 (d, *J* = 13.2 Hz, 2H), 1.95 – 1.57 (m, 4H), 1.37 – 1.21 (m, 4H). ^{13}C NMR (75 MHz, Chloroform-*d*) δ 157.97, 136.91, 87.68, 63.41, 33.69, 25.84, 25.29, 14.23. HRMS (ESI): calcd for $C_{10}H_{17}N_3SNa$: $[M + Na]^+$: *m/z* 234.10409. Found 234.1037 (1 ppm).

Synthesis of 2,3,4-tris((tert-butyldimethylsilyl)oxy)benzalde hyde (13)

t-Butyldimethylsilylchloride (1.64 g, 10.9 mmol, 3.0 equiv.) was added dropwise over 5 min to a solution of 2,3,4-trihydroxybenzaldehyde (0.5 g, 3.25 mmol, 1.0 equiv.), and diisopropylethylamine (2.5 ml, 14.6 mmol, 4.5 equiv.) in DMF (20 mL) and stirred for an additional 16 h at RT. A solution of $NaHCO_3$ (100 mL) was added and the reaction mixture was extracted with Diethyl Ether (3 x 100 ml). The combined organic layers were dried on $MgSO_4$ and concentrated under vacuo. The solid obtained was washed with cold methanol (2 x 5 mL) and cold diethyl ether (10 ml) prior to be dried under vacuo to give 1.81 g of product. Recristallisation from MeOH afforded **13** (1.37 g, 85 % yield) as a colorless cristalline powder. ^{1}H NMR (300 MHz, Chloroform-*d*) δ 10.21 (d, *J* = 0.8 Hz, 1H), 7.38 (d, *J* = 8.7 Hz, 1H), 6.62 (dd, *J* = 8.6, 0.8 Hz, 1H), 1.05 (s, 9H), 1.00 (s, 9H), 0.94 (s, 9H), 0.27 (s, 6H), 0.14 (s, 6H), 0.12 (s, 6H). HRMS (ESI): calcd for $C_{25}H_{48}O_4NaSi_3$: $[M + Na]^+$: m/z 519.27527. Found 519.2759 (1 ppm).

Synthesis of (2Z,NE)-2-(cyclohexylimino)-4-methyl-N-(2,3,4-tris((tert-butyldimethylsilyl)oxy) benzylidene)thiazol-3(2H)-amine (14)

In a small Schlenk tube equiped with a magnet stirrer, **12** (247 mg, 1.0 mmol, 1.0 equiv.) and 2,3,4-tri-(*t*-butyldimethylsilyloxy)benzaldehyd (**13**) (502 mg, 1.01 mmol, 1.0 equiv.) were dissolved in 10 mL of a 1:1 mixture of MeOH/$CHCl_3$. The orange mixture was heated at 60 °C for 2 h and the volatiles were removed under vacuo. The crude mixture was purified by column chromatography on neutral alumina with cyclohexane/diethyl ether 80:20 as eluent to give of product **14** (677 mg, 98% yield) as a brown-orange solid. FTIR (thin film) ν_{max}/cm^{-1} 2929, 2856, 1630, 1591 ; 1302, 1253, 1066, 826, 801, 757 .^{1}H NMR (300 MHz, Chloroform-*d*) δ 10.25 (s, 1H), 7.40 (d, *J* = 8.7 Hz, 1H), 6.57 (d, *J* = 8.7 Hz, 1H), 5.57 (s, 1H), 2.82 (s, 1H), 2.20 (d, *J* = 1.3 Hz, 3H), 1.90 – 1.48 – 1.14 (m, 10H), 1.06 – 0.99 (m, 17H), 0.97 (s, 9H), 0.25 (s, 6H), 0.15 (s, 6H), 0.13 (s, 6H). ^{13}C NMR (75 MHz, $CDCl_3$) δ 152.68, 150.20, 148.37, 147.46, 138.81, 137.61, 123.10, 118.40, 115.00, 90.38, 65.62, 33.18, 26.65, 26.4, 26.15, 26.00, 25.01, 18.83, 18.55, 18.52, 16.07, -3.48, -3.51, -3.92. HRMS (ESI): calcd for $C_{35}H_{64}N_3O_3Si_3SNa$: $[M + Na]^+$: *m/z* 690.39708. Found 690.3971 (0 ppm).

Synthesis of 4-((E)-(((Z)-2-(cyclohexylimino)-4-methylthiazol-3(2H)-yl)imino)methyl)benzene-1,2,3-triol 1 (FJ-809)

To a stirred solution of **14** (463 mg, 0.637 mmol, 1.0 equiv.) in MeOH (6.0 mL) was added at once $KHF_2.2H_2O$ (248 mg, 3.18 mmol, 5.0 equiv.) and left at RT for 5 h. The crude mixture was filtrated over a coton plug to discard the precipitate and rinsed with cold MeOH. Then, volatiles were removed under vacuo at r. t. and the crude mixture was purified by a short column chromatography on silica gel eluting with Chloroform/MeOH 99:1 to give product **1** (**FJ-809**) (203 mg, 92% yield) as a brown orange solid. FTIR (thin film) ν_{max}/cm^{-1} 3124, 3005, 2931, 2856, 1580, 1209, 1038, 1005, 726. ^{1}H NMR (300 MHz, Methanol-d_4) δ 9.80 (s, 1H), 6.85 (d, *J* = 8.5 Hz, 1H), 6.46 (d, *J* = 8.5 Hz, 1H), 6.16 (d, *J* = 1.4 Hz, 1H), 3.03 (m, 1H), 2.18 (d, *J* = 1.4 Hz, 3H), 1.98 – 1.87 (m, 2H), 1.83-1.81 (m, 2H), 1.67-1.63 (m, 1H), 1.53-1.28 (m, *J* = 19.2, 9.7 Hz, 5H). ^{13}C NMR (75 MHz, Methanol-d_4) δ 165.65, 158.17, 151.17, 148.70, 136.43, 132.86, 122.61, 110.54, 108.26, 95.78, 61.42, 32.10, 25.14, 24.51, 13.31. HRMS (ESI): calcd for $C_{17}H_{22}N_3O_3SNa$: $[M + Na]^+$: *m/z* 348.13764. Found 348.1377 (0 ppm).

(2Z,NE)-2-(cyclohexylimino)-4-methyl-N-(2,3,4-trimethoxy benzylidene)thiazol-3(2H)-amine (15)

In a Schlenk tube with a magnetic stirrer, **12** (32 mg, 0.12 mmol, 1.0 equiv.) and 2,3,4-trimethoxy benzaldehyde (20 mg, 0.095 mmol, 0.7 equiv.) were dissolved in 1.0 mL of MeOH. The mixture was heated at 75 °C for 12 h, filtrated through a coton plug at r.t. and volatiles evacuated under vacuo. The crude mixture was purified by column chromatography eluting with Cyclohexane/Diethyl Ether 1:1 to afford of **15** (30 mg, 92% yield) as an orange oil. FTIR (thin film) ν_{max}/cm^{-1} 2925, 2951, 1593, 1284, 1222, 1093, 804, 776^{1}H NMR (400 MHz, Chloroform-*d*) δ 10.81 (s, 1H), 7.70 (d, *J* = 8.8 Hz, 1H), 6.75 (d, *J* = 8.8 Hz, 1H), 5.60 (s, 1H), 3.94 (s, 3H), 3.91 (s, 6H), 2.94 (t, *J* = 8.1 Hz, 1H), 2.22 (s, 3H), 1.90 – 1.24 (m, 10H). ^{13}C NMR (101 MHz, $CDCl_3$) δ 154.85, 153.43, 152.33, 144.64, 142.18, 137.33, 124.24, 123.05, 120.16, 108.01, 90.83, 64.26, 61.79, 610.95, 56.18, 33.29, 225.80, 24.26, 15.85. HRMS (ESI): calcd for $C_{20}H_{27}N_3O_3SNa$: $[M + Na]^+$: *m/z* 412.16653. Found 412.1670 (1 ppm).

(2Z,NE)-2-(cyclohexylimino)-4-methyl-N-(4-nitrobenzylidene) thiazol-3(2H)-amine (16)

In a Schlenk tube with a magnet stirrer, **12** (44 mg, 0.17 mmol, 1.0 equiv.) and 4-nitrobenzaldehyde (20 mg, 0.135 mmol, 0.7 equiv.) were dissolved in 1.0 mL of MeOH. The mixture was heated at 75 °C for 2 h, filtrated through a coton plug at r.t. and the volatiles were evacuated under vacuo. Product **16** (33 mg, 71% yield) was obtained and subjected to ^{1}H NMR analysis which gave satisfactory purity. Crystals suitable for X-ray analysis were grown by layer/layer diffusion of an ethyl acetate solution of product **16** into chloroform

one. FTIR (thin film) ν_{max}/cm^{-1} 2923, 2920, 1604, 1565, 1510, 1340, 772, 684. ^{1}H NMR (300 MHz, DMSO-d_6) δ 10.65 (s, 1H), 8.28 (d, *J* = 8.8 Hz, 2H), 8.12 – 7.75 (m, 2H), 6.18 (d, *J* = 1.4 Hz, 1H), 2.89 (s, 1H), 2.20 (d, *J* = 1.3 Hz, 3H), 2.00 – 1.13 (m, 10H). ^{13}C NMR (75 MHz, DMSO) δ 152.84, 148.17, 145.21, 142.41, 136.63, 128.10, 124.56, 93.98, 64.54, 33.19, 25.92, 24.36, 15.58. HRMS (ESI): calcd for $C_{17}H_{20}N_4O_2S$: $[M + H]^+$: *m/z* 345.13797. Found 345.1383 (1 ppm).

Biology

Material &Method

FPA assay

Carboxy-fluorescein labelled peptide (5-FAM-EDIIRNIARHLAQVGDSMDR-NH_2) and Bim-WT peptide (H-Ahx-DMRPEIWIAQELRRIGDEFNAYYAR-OH) were purchased from GENEPEP and used without further purification. Mcl-1 (172-327) was produced in collaboration with Biomolecules laboratory of Pierre and Marie Curie University.[15] FPA measurements were carried out in 96-well, black, flat-bottom plates (Greiner Bio-One) using the Bioteck microplate reader Synergy 2. All assays were conducted in assay buffer containing 20mM Na_2HPO_4 (pH 7.4), 50mM NaCl, 2µM EDTA, 0.05% Pluronic F-68.[16] For IC_{50} determination, compounds were diluted in DMSO in an 8-point, serial dilution scheme, added to assay plates and were incubated with 100nM Mcl-1 for two hours. Then, to measure inhibition of Mcl-1/FAM-Bid interaction, 15nM 5-FAM-Bid peptide was added and plates were incubated for two hours at room temperature. For each experiment, a negative control containing Mcl-1 and 5-FAM-Bid peptide (equivalent to 0% inhibition), and a positive control containing Mcl-1, 5-FAM-Bid peptide, and 10µM Bim-WT peptide (equivalent to 100% inhibition), were included on each assay plate. Each point was duplicated and each experiment was performed in two biological replicates. The change in polarization was measured and used to calculate an IC_{50} (inhibitor concentration at which 50% of bound peptide is displaced), by fitting the inhibition data using GraphPad Prism 6 software to a sigmoïdal, 4PL, X is log(concentration). This was converted into a binding dissociation constant (Ki) according to the formula described by Nikolovska-Coleska *et al.*[17]

Cell culture and treatment

IGROV1-R10 cell line was established as described previously[18] from the IGROV1 cell line, itself kindly provided by Dr. Jean Bénard (Institut Gustave Roussy, Paris, France). It was grown in RPMI1640 (Gibco) medium supplemented with 2 mM Glutamax™, 25mM HEPES (4-(2-hydroxyethyl)-1-piperazine-ethanesulfonic acid), 10% decomplemented FBS (Fetal Bovine Serum) (Gibco) and 33mM sodium bicarbonate (Gibco) and maintained in a 5% CO_2 humidified atmosphere at 37 °C. Ovarian cancer cell line was certified mycoplasma-free thanks to a MycoAlert test. Cells were seeded in 25 cm2 flasks 24 hours before their treatment and exposed to **MIM1** or **FJ-809** as single agents or in combination with ABT-737 or S63845 for 24 hours at the indicated concentrations.

Nuclei staining by DAPI

After treatment, both detached and adherent cells were pooled after trypsinization, applied to a polylysine-coated glass slide by cytocentrifugation and fixed with a solution of ethanol/chloroform/acetic acid (6:3:1). The preparations were then incubated for 15min at room temperature with 1µg/ml DAPI solution (Boehringer Mannheim-Roche, Mannheim, Germany), washed in distilled water, mounted under a coverslip in Mowiol (Calbiochem) and analysed under a fluorescence microscope (BX51, Olympus, Rungis, France).

On each image a deep-learning-based method of 2D nucleus detection was applied [Uwe Schmidt, Martin Weigert, Coleman Broaddus, and Gene Myers. Cell Detection with Star-convex Polygons. International Conference on Medical Image Computing and Computer-Assisted Intervention [MICCAI, Granada, Spain, September 2018] with a python program. A size filter was used to class intact nuclei and fragmented nuclei. Then, a closing morphological operator was applied to regroup the clusters of small fragments. Each cluster was counted as one fragmented nucleus.

DNA content analysis by flow cytometry

After treatment, both detached and adherent cells were pooled after trypsinization, washed with 1X PBS and fixed with ethanol 70°. Cells were centrifuged at 2000 rpm for 5 min and incubated for 30 min at 37°C in PBS to allow the release of low-molecular weight DNA (characteristic of apoptotic cells). Cell pellets were stained with propidium iodide (PI) using the DNA Prep Coulter Reagent Kit (Beckman-Coulter, Villepinte France). Samples were thereafter analysed using a Gallios flow cytometer (Beckman-Coulter) and cell cycle distribution was determined using Kaluza acquisition software (Beckman-Coulter).

Western blot analyses

After treatment, both detached and adherent cells were pooled after trypsinization. Cells were rinsed with ice-cold PBS, suspended in a lysis buffer [RIPA : NaCl 150mM, Tris (pH 8) 50mM, Triton X100 1%, PMSF 4mM, EDTA 5mM, NaF 10mM, NaPPi 10mM, Na_3OV_4 1mM, aprotinin 0.5µL/mL and 4.6 mL ultra-pure water] and incubated on ice for 30min. Lysates were collected after centrifugation (13200g, 10 min, 4°C) and protein concentrations were determined using the Bradford assay (Bio-Rad, Hercules, USA). 25µg of protein were separated by SDS–PAGE on a 4-15% gradient polyacrylamide gel (Invitrogen, Cergy-Pontoise, France) and transferred to Hybond-PVDF membranes (Amersham, Orsay, France). After blocking non-specific binding sites for 1 hour at RT by 5% (w/v) non-fat dry milk in

TBS with 0.1% (v/v) Tween20 (T-TBS), the membranes were incubated overnight at 4°C with the following rabbit monoclonal antibody: PARP, caspase-3 (Cell Signaling Technology, Ozyme, Saint-Quentin-en-Yvelines, France) or mouse monoclonal antibody: actin (EMD, Millipore, France). Membranes were then washed with T-TBS and incubated for 1 hour with the appropriate horseradish peroxidase-conjugated anti-rabbit (Cell Signaling Technology, France) or anti-mouse (Amersham, Orsay, France) secondary antibodies. Revelation was performed exposing membranes to Clarity Max Western ECL Substrate (BioRad #1705062) using a luminescent Image Analyzer (GE Healthcare, Orsay, France).

Molecular modelling

Material &Method

We used a two-step protocol for molecular docking. First, a raw complex was obtained with Glide, using the standard precision mode (enhanced sampling for ligand conformers, enhanced planarity for conjugated π-group, post-docking minimization and strain correction term for final scoring). Then an induced-fit docking was performed with the best Glide pose, refining amino acids located within 7 Å of the ligand. The OPLS3e force field was used, with redocking in the standard precision mode. Finally, MM-GBSA was calculated on the final pose (VSGB solvation model and OPLS3e force field). Molecular dynamics experiments were a three-step process: after insertion of the Mcl-1/**MIM1** or Mcl-1/**FJ-809** complex in a solvent box (2 Cl^- and nearly 8600 water molecules), (i) energy minimization for 0.3 ns with restraints for protein and ligand (only ions and water were allowed to move (ii) 0.1 ns equilibration in NPT conditions (300 K, 1 bar), using the RESPA integrator (2 fs / 6 fs time steps for near / far atoms), and a cut-off radius of 9 Å for Coulombic interactions, keeping only protein backbone restraints (iii) production for 1 µs in the same conditions, without any restraint. Molecular dynamics and RDF calculation were performed with Desmond, as implemented in Maestro v. 12.4 (Schrödinger LLC, San Diego, CA). The Mcl-1 structure PDB:3KJ0 was used for all simulations.[19]

Conclusions

In summary we have designed a strategy to prepare unambiguously molecules with a thiazol-3(2H)-yl)imino core, exemplified here by the synthesis of the **FJ-809** compound (**1**) which has the structure originally ascribed to **MIM1** (**2**). Biological studies demonstrated that this molecule **FJ-809** is not an inhibitor of the anti-apoptotic protein Mcl-1, contrary to **2**, and these results have been confirmed by FPA assays. Extensive molecular modelling and molecular dynamic studies have been performed to understand the higher affinity of **MIM1** (**2**) for Mcl-1.

Conflicts of interest

There are no conflict of interest to declare.

Acknowledgments

We thank CNRS and University of Rennes 1 for their support. Financial support by the "Ligue contre le Cancer, Conseil Interrégional Grand Ouest" and "Ligue Contre le Cancer, Conseil Interrégional de Normandie et Comité du Calvados" are gratefully acknowledged. This work was also supported by the "Conseil Régional de Normandie" and European Union (The ONCOTHERA European project "Normandy Network for innovative therapeutics in oncology" which is co-funded by the Normandy County Council, the European Union within the framework of the Operational Programme ERDF/ESF 2014-2020), by the French State (CPER Innovons 2), the University of Caen Normandie and Inserm. We are very grateful to the Centre Régional de Mesures Physiques de l'Ouest, Rennes (CRMPO) team for the HRMS analyses plus various NMR studies and for very fruitful discussions. We thank European FEDER funds for acquisition of D8Venture X-ray diffractometer used for crystal structure determination. HP is recipient of a doctoral fellowship from the "Ministère de l'Enseignement Supérieur, de la Recherche et de l'Innovation" granted by Normandy Doctoral School 497 "EDN Bise". We acknowledge Maryline Guillamin (Flow cytometry accommodation, SF 4206 ICORE, University of Caen Normandie), for her helpful technical support and Pr Marc-André Mahé, head of the Comprehensive Cancer Center François Baclesse (Caen, France), for his constant support.

Notes and References.

1 Ferlay J, Ervik M, Lam F, Colombet M, Mery L, Piñeros M, et al. Global Cancer Observatory: Cancer Today. Lyon: International Agency for Research on Cancer; 2020 (https://gco.iarc.fr/today, accessed August 2021).

2 D. Hanahan and R. A. Weinberg, *Cell*, 2011, **144**, 646-674.

3 A. N. Hata, J. A. Engelman and A. C. Faber, *Cancer Discovery*, 2015, **5**, 475-487.

4 L. M. Juarez-Salcedo, V. Desai and S. Dalia, *Drug Context*. 2019, Oct 9;8:212574.

5 H. Wang, M. Guo, H. Wei and Y. Chen, *J Hematol. Oncol*., 2021, **14**: 67.

6 S. Fletcher, *Expert Opin. Ther. Pat.*, 2019, 29, 909-919.

7 For selected recent reviews see: (a) M. J. Roy, A. Vom, P. E. Czabotar and G. E. Lessene, *Brit. J. Pharmacol.*, 2014, **171**, 1973-1987; (b) J. Belmar and S. W. Fesik, *Pharmacol. & Therapeutics* 2015, **145**, 76-84; (c) E. J. Hennessy, *Bioorg. Med. Chem. Lett*. 2016, **26**, 2105-2114; (d) J. L. Yap, L. Chen, M. E. Lanning and S. Flechter, *J. Med. Chem.*, 2017, **60**, 821-838; (e) A. Ashkenazi, W. J. Fairbrother, J. D. Leverson and A. J. Souers, *Nat. Rev. Drug Discov.*, 2017, **16**, 273-284; (f) C. Denis, J. Sopkova-de Oliveira Santos, R. Bureau, and A. S. Voisin-Chiret, *J. Med. Chem.* 2020, **63**, 928−943; (g) K. Li, *Bioorg. Med. Chem. Lett.* 2021, **32**, 127717; (h) A. Negi and P. V. Murphy, *Eur. J. Med. Chem.* 2021, **210**, 113038 and references cited therein.

8 (a) N. A. Cohen, M. L. Stewart, E. Gavathiotis, J. L. Tepper, S. R. Bruekner, B. Koss, J. T. Opferman and L. D. Walensky, *Chem Biol*, 2012, **19**, 1175-1186; (b) L. D. Walensky, Patent WO2013/142281, 2013.
9 H. Paysant, S. Hedir, F. Justaud, L.-B. Weiswald, A. Nasr El Dine, A. Soulieman, A. Hachem, N. Elie, E. Brotin, C. Denoyelle, J. Bignon, F. Roussi, M. Jouanne, O. Tasseau, T. Roisnel, A.- S. Voisin-Chiret, R. Grée, N. Levoin and L. Poulain, *Org. Biomol. Chem.* 2021, **19**, 8968-8987.
10 (a) S. Murru, C. B. Singh, V. Kavala and B. K. Patel, *Tetrahedron*, 2008, **64**, 1931-1942.(b) S. M. Abou Seri, N. A. Farag and G. S. Hassan, *Chem Pharm Bull (Tokyo)*, 2011, **59**, 1124-1132. (c) M. M. Heravi and S. Moghimi, *Tetrahedron Lett*, 2012, **53**, 392-394. (c) T. W. Sanchez, B. Debnath, F. Christ, H. Otake, Z. Debyser and N. Neamati, *Bioorg Med Chem*, 2013, **21**, 957-963. (d) W.-D. Pfeiffer, D. Junghans, A. S. Saghyan and P. Langer, *J. Heterocyclic Chem,* 2014, **51**, 1063-1067. (e) K. M. Khan, S. Qurban, U. Salar, M. Taha, S. Hussain, S. Perveen, A. Hameed, N. H. Ismail, M. Riaz and A. Wadood, *Bioorg Chem*, 2016, **68**, 245-258. (f) U. Salar, M. Taha, K. M. Khan, N. H. Ismail, S. Imran, S. Perveen, S. Gul and A. Wadood, *Eur J Med Chem*, 2016, **122**, 196-204. (g) S. Mirza, S. Asma Naqvi, K. Mohammed Khan, U. Salar and M. I. Choudhary, *Bioorg Chem*, 2017, **70**, 133-143. (h) C. Bodhak and A. Pramanik, *J Org Chem*, 2019, **84**,7265 7278. (h) A. A. Hassan, N. K. Mohamed, A. A. Aly, H. N. Tawfeek, S. Bräse and M. Nieger, *J Mol Struct*, 2019, **1176**, 346-356.
11 (a) N. Karali, A. Kocabalkanli, A. Gürsoy and O. Ateş, *Farmaco*, 2002, **57**, 589-593. (b) M. C. Cardia, S. Distinto, E. Maccioni, A. Plumitallo, M. L. Sanna, M. Saddi and A. Delogu, *J Heterocycl Chem*, 2006, **43**, 1337-1342. (c) S. Y. Abbas, A. A. Farag, Y. A. Ammar, A. A. Atrees, A. F. Mohamed and A. A. El-Henawy, *Monatsh Chem*, 2013, **144**, 1725-1733. (d) W.-D. Pfeiffer, K.-D. Ahlers, A. S. Saghyan, A. Villinger and P. Langer, *Helv Chim Acta*, 2014, **97**, 76-87. (e) S. N. Eman, M. E.-H. Salwa and R. Z. Eman, *Int J Pharm Pharm Sci*, 2015, **7**. (f) R. Meleddu, S. Distinto, A. Corona, E. Tramontano, G. Bianco, C. Melis, F. Cottiglia and E. Maccioni, *J Enzym Inhib Med Chem*, 2017, **32**, 130-136. (g) T. I. de Santana, M. O. Barbosa, P. Gomes, A. C. N. da Cruz, T. G. da Silva and A. C. L. Leite, *Eur J Med Chem*, 2018, **144**, 874-886. (h) M. A. Hussein, A. H. Kafafy, S. G. Abdel-Moty and O. M. Abou-Ghadir, *Acta Pharm*, 2009, **59**, 365-382.
12 D. J. Chaplin; K. Edvardsen; K. G. Pinney; J. A. Prezioso; M.Wood, WO2004078126 A2, 2004.
13 CCDC 2123510 (for compound **16**), contain the supplementary crystallographical data for this paper. These data can be obtained free of charge from the Cambridge Crystallographic Data Centre (CCDC), 12 Union Road, Cambridge CB2 1EZ, UK; fax, +44(0) 1223 336 033; e-mail: deposit@ccdc.cam.ac.uk
14 (a) N. Bharti, K. Husain, M. T. Gonzalez Garza, D. E. Cruz-Vega, J. Castro-Garza, B. D. Mata-Cardenas, F. Naqvi and A. Azam, *Bioorg. Med. Chem. Lett.* 2002, **12**, 3475–3478; (b) S. M. Basheer, A. C. Willis, R. J. Pace and A. Sreekanth, *Polyhedron*, 2016, **109**, 7-18.
15 A. Friberg, D. Vigil, B. Zhao, R. N. Daniels, J. P. Burke, P. M. Garcia-Barrantes, D. Camper, B. A. Chauder, T. Lee, E. T. Olejniczak and S. W. Fesik, *J Med Chem*, 2013, **56**, 15-30.
16 S. Desrat, C. Remeur and F. Roussi, *Org Biomol Chem*, 2015, **13**, 5520-5531.
17 Z. Nikolovska-Coleska, R. Wang, X. Fang, H. Pan, Y. Tomita, P. Li, P. P. Roller, K. Krajewski, N. G. Saito, J. A. Stuckey and S. Wang, *Anal Biochem*, 2004, **332**, 261-273.
18 L. Poulain, H. Lincet, F. Duigou, E. Deslandes, F. Sichel, P. Gauduchon and C. Staedel, *Int J Cancer*, 1998, **78**, 454-463.
19 E. Fire, S. V. Gulla, R. A.Grant and A. E Keating, *Protein Sci*, 2010, **19**, 507-519.